

Simulating Aqueous-Phase Isoprene-Epoxydiol (IEPOX) Secondary Organic Aerosol Production During the 2013 Southern Oxidant and Aerosol Study (SOAS)

Sri Hapsari Budisulistiorini,^{†,‡,§} Athanasios Nenes,^{||,⊥,♯,∇} Annmarie G. Carlton,[○] Jason D. Surratt,[‡] V. Faye McNeill,^{*,◆} and Haval O. T. Pye^{*,†}

[†]National Exposure Research Laboratory, U.S. EPA, Research Triangle Park, North Carolina 27711, United States

[‡]Department of Environmental Sciences and Engineering, Gillings School of Global Public Health, University of North Carolina, Chapel Hill, North Carolina 27599, United States

[§]Earth Observatory of Singapore, Nanyang Technological University, Singapore 639798, Singapore

^{||}School of Earth and Atmospheric Sciences, Georgia Institute of Technology, Atlanta, Georgia 30322, United States

[⊥]School of Chemical and Biomolecular Engineering, Georgia Institute of Technology, Atlanta, Georgia 30322, United States

[♯]Institute of Chemical Engineering Sciences, Foundation for Research and Technology - Hellas, Patras GR-26504, Greece

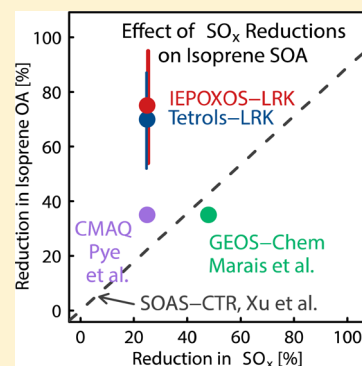
[∇]Institute of Environmental Research and Sustainable Development, National Observatory of Athens, Palea Penteli GR-15236, Greece

[○]Department of Chemistry, University of California, Irvine, California 92617, United States

[◆]Department of Chemical Engineering, Columbia University, New York, New York 10027, United States

Supporting Information

ABSTRACT: The lack of statistically robust relationships between IEPOX (isoprene epoxydiol)-derived SOA (IEPOX SOA) and aerosol liquid water and pH observed during the 2013 Southern Oxidant and Aerosol Study (SOAS) emphasizes the importance of modeling the whole system to understand the controlling factors governing IEPOX SOA formation. We present a mechanistic modeling investigation predicting IEPOX SOA based on Community Multiscale Air Quality (CMAQ) model algorithms and a recently introduced photochemical box model, simpleGAMMA. We aim to (1) simulate IEPOX SOA tracers from the SOAS Look Rock ground site, (2) compare the two model formulations, (3) determine the limiting factors in IEPOX SOA formation, and (4) test the impact of a hypothetical sulfate reduction scenario on IEPOX SOA. The estimated IEPOX SOA mass variability is in similar agreement ($r^2 \sim 0.6$) with measurements. Correlations of the estimated and measured IEPOX SOA tracers with observed aerosol surface area ($r^2 \sim 0.5-0.7$), rate of particle-phase reaction ($r^2 \sim 0.4-0.7$), and sulfate ($r^2 \sim 0.4-0.5$) suggest an important role of sulfate in tracer formation via both physical and chemical mechanisms. A hypothetical 25% reduction of sulfate results in $\sim 70\%$ reduction of IEPOX SOA formation, reaffirming the importance of aqueous phase chemistry in IEPOX SOA production.



INTRODUCTION

Particles with aerodynamic diameters less than $2.5 \mu\text{m}$ ($\text{PM}_{2.5}$) are known to affect human health and regional climate forcing.¹ Organic aerosol (OA) constitutes a large fraction of $\text{PM}_{2.5}$ mass.² In summer, biogenic secondary organic aerosol (SOA) is a major fraction of OA and plays an important role in the spatial and temporal distribution of aerosol optical thickness, potentially causing regional cooling over the southeastern United States.³⁻⁵

Isoprene (2-methyl-1,3-butadiene) emission is estimated to be 600 Tg yr^{-1} ,⁶ which makes it the most abundant nonmethane volatile organic compound (VOC) emitted globally. It also plays a substantial role in SOA production.⁷ On average, isoprene-derived SOA tracers account for up to

20% of total OA observed in the southeastern U.S. (SE US), and compounds derived from isoprene epoxydiol (IEPOX) chemical pathways can account for $>95\%$ of isoprene SOA.^{8,9} IEPOX-OA, a positive matrix factor linked to IEPOX-derived SOA (IEPOX SOA) tracers, comprises one-third of ambient organic aerosol mass in urban and rural areas in the SE US,⁹⁻¹¹ suggesting a regional source. Among isoprene-derived SOA tracers, 2-methyltetrols (tetrols) and their sulfate ester derivatives (organosulfates) contribute $\sim 33\%$ and $\sim 34\%$ of

Received: November 15, 2016

Revised: April 7, 2017

Accepted: April 10, 2017

Published: April 10, 2017

IEPOX-OA, respectively, at the Look Rock (LRK), Tennessee site.⁹

Inclusion of biogenic and anthropogenic SOA precursors and mechanisms in the Community Multiscale Air Quality (CMAQ) model improves the temporal correlation between predicted and semiempirical secondary organic carbon (OC).¹² Addition of the acid-catalyzed reactive uptake mechanism of IEPOX into CMAQ further improves predictions of tetrols against field measurements.¹³ Using the updated SOA module in the CMAQ model, Karambelas et al.¹⁴ reported a strong correlation between predicted and observed IEPOX SOA, although the simulations underestimate the measurements by an order of magnitude.

McNeill et al.¹⁵ introduced GAMMA (Gas-Aerosol Model for Mechanism Analysis), a detailed photochemical box model of aqueous-aerosol SOA (aaSOA) formation. A version of GAMMA with simplified aqueous reaction mechanism, simpleGAMMA, has been shown to be computationally efficient and suitable for coupling with large-scale atmospheric chemistry models.¹⁶ The aqueous aerosol phase mechanism in simpleGAMMA treats SOA formation from glyoxal and IEPOX.

IEPOX-derived organosulfates (IEPOXOS) and tetrols, which have been quantified in laboratory experiments,^{17,18} have been shown to contribute up to half of all known IEPOX-derived aerosol-phase species in the southeastern U.S.^{8,9} The accepted formation pathway for IEPOX SOA is through acid-catalyzed ring-opening reactions of isoprene epoxides in concert with nucleophilic addition in aqueous particles.^{18–20} An airborne study over the southeastern U.S. found a strong dependency between IEPOXOS and acidic sulfate aerosol.²¹ However, ground-based studies in the eastern US suggest weak or no correlation between IEPOX SOA and aerosol pH or liquid water content (LWC), but a positive correlation with sulfate.^{9,11} Additionally, a preliminary modeling study employing simpleGAMMA found good correlation ($r^2 \sim 0.6$) between estimated IEPOX SOA and measurements made during the 2013 Southern Oxidant Aerosol Study (SOAS) campaign.⁹

This study aims to investigate the formation of two IEPOX SOA tracers, IEPOXOS and tetrols, using CMAQ and simpleGAMMA algorithms, and evaluate the model response to perturbations that replicate atmospheric conditions. Predictions from these two different algorithms are compared with measurement results from the 2013 SOAS campaign. Only two IEPOX SOA tracers are predicted and investigated by these algorithms since they are the most abundant tracers during the entire field observation.⁹ Limiting factors in IEPOX SOA formation are investigated and the IEPOX SOA response due to changes in SO_x emission were estimated.

MATERIALS AND METHODS

Two different representations of IEPOX SOA formation were implemented in box-model form, namely CMAQ-box and simpleGAMMA, using conditions representative of the SOAS Look Rock (LRK) site.

CMAQ-box. CMAQ-box is based on the algorithms in the CMAQ model, which are detailed in the work of Pye et al.¹³ Briefly, CMAQ treats IEPOX SOA formation as heterogeneous uptake of gaseous IEPOX into the aerosol phase as a first order reaction:



Governed by a first order heterogeneous rate constant, k_{het} ²² such that

$$\frac{d[\text{IEPOX}]}{dt} = -k_{\text{het}}[\text{IEPOX}] \quad (1)$$

where

$$k_{\text{het}} = \frac{SA}{\frac{r_p}{D_g} + \frac{4}{\nu\gamma}} \quad (2)$$

SA is the aerosol surface area ($\mu\text{m}^2 \text{cm}^{-3}$) upon which uptake occurs, ν is the mean molecular speed (m s^{-1}) in the gas phase, and r_p is the effective particle radius (cm). D_g is the diffusivity of IEPOX in the gas phase, which is estimated as $D_g = 1.9 \text{ cm}^2 \text{s}^{-1} (\text{MW})^{-2/3}$, with MW as molecular weight (g mol^{-1}).¹⁵ The heterogeneous reaction is parameterized using a reactive uptake coefficient (γ) calculated with the following.^{23,24}

$$\frac{1}{\gamma} = \frac{1}{\alpha} + \frac{\nu}{4H^*RT\sqrt{D_a k_{\text{particle}}}} \frac{1}{\coth(q) - 1/q} \quad (3)$$

Here, α is the accommodation coefficient (0.02),¹⁵ H^* is the Henry's Law coefficient (M atm^{-1}), R is the gas constant, T is temperature (K), D_a is diffusivity in the aerosol phase ($1 \times 10^{-9} \text{ m}^2 \text{s}^{-1}$),²⁵ q is the diffuso-reactive parameter ($r_p\sqrt{k_{\text{particle}}/D_a}$), and k_{particle} is the pseudo-first order rate constant (s^{-1}) for reaction of IEPOX in the aerosol phase. This formulation allows for the model to predict whether the particle-phase reaction will occur throughout the particle, or as a surface process based on the relative time scales for reaction ($1/k_{\text{particle}}$) vs aerosol-phase diffusion (r_p^2/D_a). The Henry's law coefficient was set to $3 \times 10^7 \text{ M atm}^{-1}$ based on the value measured by Nguyen et al. and used in CMAQ starting with v5.2²⁶ and simpleGAMMA v1.0.¹⁶

simpleGAMMA. A detailed description of simpleGAMMA is available in Woo and McNeill.¹⁶ Briefly, simpleGAMMA represents IEPOX SOA in terms of aqueous uptake followed by aqueous-phase reaction²³ to form IEPOX SOA consisting of tetrols and IEPOXOS:



Formation of the aaSOA of IEPOX SOA (mol L^{-1} of aerosol) is given by

$$\frac{d[\text{IEPOXSOA}]}{dt} = \frac{k_{\text{mt,IEPOX}}}{RT} P_{\text{IEPOX}} - \frac{k_{\text{mt,IEPOX}}}{H^*RT} [\text{IEPOX}_{(aq)}] + \sum_k r_{k,\text{aq}} \quad (4)$$

where, P_{IEPOX} is the gas-phase partial pressure of species IEPOX. $r_{k,\text{aq}}$ are the rates of formation or decomposition of IEPOX due to chemical reactions in aerosol phase ($r_{k,\text{aq}} = k_{\text{particle}}[\text{IEPOX}_{(aq)}]$). $k_{\text{mt,IEPOX}}$ is the gas-to-aerosol mass transfer coefficient of IEPOX, which can be described as follows:¹⁶

$$k_{\text{mt,IEPOX}} = \frac{1}{\frac{r_p^2}{3D_g} + \frac{4r_p}{3\nu\alpha}} \quad (5)$$

Particle-Phase Reaction Parameters. The particle-phase reaction rate constant for IEPOX is calculated assuming protonation of the epoxide oxygen and nucleophilic addition in both CMAQ and simpleGAMMA following an A2 mechanism by Eddingsaas et al.¹⁹ While CMAQ does not treat NH_4^+ as an acid for epoxide uptake purposes, we implemented k_{particle} such that it was the same in both

Table 1. Rate Constants for Aqueous Aerosol IEPOX SOA Formation Catalyzed by H⁺, HSO₄⁻, and NH₄⁺ in CMAQ-box and simpleGAMMA

| species | nucleophile added | $k_{i,H^+} [M^{-2} s^{-1}]$ | $k_{i,HSO_4^-} [M^{-2} s^{-1}]$ | $k_{i,NH_4^+} [M^{-2} s^{-1}]$ |
|------------------|-------------------|-----------------------------|---------------------------------|--------------------------------|
| 2-methyltetrols | water | 9.00×10^{-4a} | 1.31×10^{-5a} | 3.10×10^{-7b} |
| IEPOX-derived OS | sulfate | 1.27×10^{-3c} | | |

^aEddingsaas et al.¹⁹ ^bNguyen et al.²⁹ ^cBased on tetrols: IEPOXOS ratio from Riedel et al.²⁷

simpleGAMMA and CMAQ-box calculations using the most recent values from literature which included updating the organosulfate formation rate constant following Riedel et al.²⁷ Thus, the particle-phase rate constant for both CMAQ and simpleGAMMA simulations in this study is

$$k_{\text{particle}} = k_{H^+, \text{water}} a_{H^+} \text{LWC} + k_{\text{HSO}_4^-, \text{water}} [\text{HSO}_4^-] \text{LWC} + k_{\text{NH}_4^+, \text{water}} [\text{NH}_4^+] \text{LWC} + k_{H^+, \text{SO}_4^{2-}} a_{H^+} [\text{SO}_4^{2-}] \quad (6)$$

a_{H^+} is the proton activity which represents aerosol acidity. ISORROPIA-II²⁸ was used to estimate a_{H^+} as well as nucleophile concentrations (SO_4^{2-} , HSO_4^- , NH_4^+ , and LWC in mol L⁻¹ of aerosol) based on aerosol species (SO_4^{2-} , NO_3^- , Cl^- , and NH_4^+ in $\mu\text{mol m}^{-3}$) measured at the LRK site by an Aerodyne Aerosol Chemical Speciation Monitor (ACSM) and ammonia from the Ammonia Monitoring Network (AMoN) (Supporting Information (SI) Table S1). Updating the particle-phase reaction scheme to include NH_4^+ protonation reaction with IEPOX²⁹ does not significantly change (increase by 5%) prediction of k_{particle} (SI Figure S1). The resulting nucleophile concentration used as input to the box models is not the same as the ACSM measured values since the estimation considers the contribution of inorganic ions (e.g., NO_3^- , NH_4^+ , etc.) and organics to total aqueous-phase aerosol particle volume in the air (SI Figure S2).

All particles were assumed to consist of one internally mixed organic–inorganic phase consistent with the dominant phase state for highly oxygenated organic aerosol in a humid environment;^{26,30} indeed RH is high enough (0.77 ± 0.10) at LRK so that phase separation is unlikely to occur, and pH is considered to be homogeneous across the aerosol particle volume.³¹ Aerosol water was estimated based solely on the uptake from inorganic species using ISORROPIA-II and used as input to CMAQ-box and simpleGAMMA. Organic water was not considered in the calculations owing to the unavailability of organic aerosol water (or hygroscopicity) measurements. Water associated with organic species could contribute 35% of total aerosol water in southeastern US^{11,31} (especially during nighttime) and modulate aerosol pH by $\sim 6\%$,³¹ compared to only considering inorganic-associated aerosol water. This effect, although a source of uncertainty (for acidity and other species concentration), does not modulate aerosol water more than 2-fold (SI Figure S3) nor considerably affect the correlations between SOA tracers and particle volume (SI Table S2). Therefore, considering only aerosol water associated with inorganic aerosol species is sufficient for our study.

The ISORROPIA-II outputs as well as other parameters described in SI Table S1 are used in the base case simulation of IEPOXOS and tetrol formation. SOA tracer mass formed over 12 and 6 h of aqueous processing is compared with measurements from Budisulistiorini et al.⁹ briefly described in the following subsection. The rate constants for catalysis by H⁺, HSO₄⁻, and NH₄⁺ used in CMAQ and simpleGAMMA are provided in Table 1. Repartitioning of tracers back to the gas phase is not considered in this study. Organosulfates are

expected to have very low volatility, with a vapor pressure of 1.7×10^{-8} Torr at ambient temperature (estimated using eqs 1 and 2 by Li et al.³²). There is considerable uncertainty surrounding the gas-particle partitioning of tetrols.³³ Although they are relatively semivolatile in pure form (vapor pressure of 1.6×10^{-5} Torr³⁴), they are observed in unexpectedly high concentrations in ambient particles, and their partitioning cannot be described using equilibrium models, pointing to an unquantified potential role of in-particle oligomer formation.³⁵ In light of this uncertainty, they are assumed to be nonvolatile in the model calculations in this work.

The speciation of IEPOX SOA between tetrols and IEPOXOS in both models was determined based on the relative rates of precursor conversion to tetrols and IEPOXOS. Specifically,

$$\text{IEPOXSOA} = \beta \times \text{IEPOXOS} + (1 - \beta) \text{tetrols} \quad (7)$$

where β is the fraction of products resulting in an organosulfate and is as follows

$$\beta = \frac{k_{H^+, \text{SO}_4^{2-}} a_{H^+} [\text{SO}_4^{2-}]}{k_{\text{particle}}} \quad (8)$$

This relative rate of tracer formation holds provided conversion of IEPOXOS to tetrols is slow.

Field Measurements. Field measurements at the SOAS LRK ground site provided inputs for the model simulations and IEPOX SOA tracer concentrations for model evaluation. Ambient temperature, RH and aerosol concentrations were obtained from measurements⁹ and summarized in SI Table S1. The sum of IEPOX and its gas-phase precursor ISOPOOH were detected as $[\text{CH}_3\text{COO} \cdot \text{C}_5\text{H}_{10}\text{O}_3]^-$ ion at m/z 177 by an Aerodyne high-resolution time-of-flight chemical ionization mass spectrometry (HR-ToF-CIMS) using acetate reagent ion chemistry. As reported in Budisulistiorini et al.,⁹ the instrument had similar sensitivities toward both gaseous compounds, which allowed us to estimate the IEPOX concentration as

$$\text{IEPOX} = \frac{m/z177 \text{ signal}}{1 + b} \quad (9)$$

where b is the concentration of ISOPOOH relative to IEPOX predicted by Weather Research and Forecasting Community Multiscale Air Quality (WRF-CMAQ) for LRK³⁶ as a function of hour of day (SI Table S3).

Tetrols and IEPOXOS were quantified during the 2013 SOAS campaign at the LRK ground site and details are available in Budisulistiorini et al.⁹ Briefly, PM_{2.5} samples were collected onto prebaked Tissuquartz filters (Pall Life Sciences, 8 × 10 in) with three high-volume PM_{2.5} samplers (Tisch Environmental, Inc.). Each sampler collected PM_{2.5} every 3 h during the high-NO_x and SO_x periods (intensive sampling periods), and every 11 h during the low-NO_x and SO_x periods (regular sampling periods). From each filter two 37 mm punches were extracted in separate precleaned scintillation vials with 20 mL high-purity methanol (LC-MS Chromasolv-grade,

Sigma-Aldrich) by sonication for 45 min. One punch was used for analysis by gas chromatography interfaced to an electron impact-mass spectrometer (GC/EI-MS) and the other one was used for ultra performance liquid chromatography coupled to both diode array detection and high-resolution quadrupole time-of-flight electrospray ionization mass spectrometry (UPLC/DAD-ESI-HR-QTOFMS).

Tetrol concentrations were analyzed by GC/EI-MS (Hewlett-Packard (HP) 5890 Series II Gas Chromatograph equipped coupled to an HP 5971A Mass Selective Detector) with prior trimethylsilylation of filter extracts by reaction with 100 μL of BSTFA + TMCS (99:1, v/v, Supelco) and 50 μL of pyridine (anhydrous, 99.8%, Sigma-Aldrich) at 70 $^{\circ}\text{C}$ for 1 h. Tetrols were quantified using authentic standards synthesized in-house.⁹

IEPOXOS concentrations were analyzed by UPLC/DAD-ESI-HR-QTOFMS (Agilent 6500 series system equipped with a Waters Acquity UPLC HSS T3 column) with prior reconstitution of filter residues in 150 μL of a 50:50 (v/v) solvent mixture of methanol (LC-MS Chromasolv-grade, Sigma-Aldrich) and laboratory Milli-Q water (18.2 M Ω). IEPOXOS were quantified using an authentic standard synthesized in-house.⁹

Sensitivity Simulations. We performed sensitivity simulations to examine the effects of atmospheric processing time on the concentration of predicted tetrols and IEPOXOS. Processing times of 12 and 6 h provide bounds on the amount of time needed in the atmosphere for IEPOX to produce SOA and fall within the range of PM_{2.5} sampling time. However, if the Henry's Law coefficient for IEPOX were higher, as measured by Gaston et al. ($1.7 \times 10^8 \text{ M atm}^{-1}$), or lower, as predicted by HenryWin (Pye et al.,¹³ $2.7 \times 10^6 \text{ M atm}^{-1}$) the processing time required to produce a given concentration of tracer would be shorter or longer, respectively. Thus, it is not possible for us to separate the effects of processing time from Henry's Law coefficient in a robust way.

To examine the potential model sensitivity of IEPOX SOA formation to SO₂ emissions, sulfate mass concentrations in the model were reduced by 25%.³⁷ The other conditions (i.e., total ammonia, RH, temperature) remained similar to the base case. ISORROPIA-II was used to propagate the effects of the reduced total sulfate concentration on the concentrations of acids (H⁺, NH₄⁺, and HSO₄⁻) and LWC. The effect of reduced mass on volume and SA was also propagated using the expected changes in mass. These were then used as input to CMAQ-box and simpleGAMMA.

RESULTS AND DISCUSSION

Tracers Estimation and Comparison to Observations.

CMAQ-box and simpleGAMMA predict variability in IEPOX SOA formation well, as indicated by good correlation ($r^2 \sim 0.6$) of predicted tracer concentrations with the measurements (Figure 1). In this study, the 12 h processing time is assumed to reflect atmospheric photooxidation time during a day, while short processing times are consistent with observations of IEPOX SOA in the southeast U.S. that have shown diurnal trends reach a maximum around noon.^{9,10} Figure 1 shows that 12 h processing time in both CMAQ and simpleGAMMA results in an overestimation of the sum of tetrol and IEPOXOS mass by a factor of 2–3. A closer mass agreement of estimated vs observed IEPOX SOA tracers is achieved when the model processing time of aaSOA is shorter at 6 h (SI Table S4). While processing time does not affect the correlation between

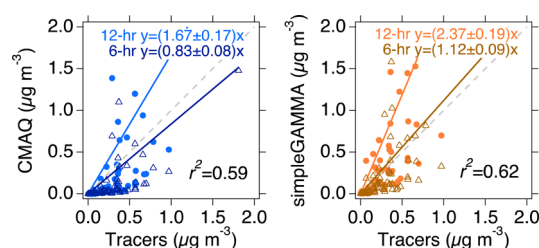


Figure 1. Comparison of sum of SOA tracers (i.e., IEPOXOS and tetrols) estimated by models (simpleGAMMA and CMAQ-box) with measurements during 2013 SOAS. 12 h simulation results are depicted as solid circles, whereas 6 h simulation results are shown in open triangles. Shorter simulation time resulted in lower slopes but no change in correlation values.

predictions and observations for each model, it affects the magnitude of model predictions. At an integration time of 12 h, CMAQ-box overpredicts tetrol mass (slope = 2.3, SI Table S4), and under-predicts IEPOXOS (slope = 0.7). For simpleGAMMA, tetrol mass is overpredicted (slope = 3.25) and IEPOXOS is estimated well (slope ~ 1). By reducing the integration to 6 h, both models underpredict IEPOXOS mass (slope = 0.4–0.5, SI Table S4, Figure 2), but better estimate tetrol mass (slope = 1–1.5). The overestimation of tetrols might be attributed to repartitioning to and/or production in the gas phase^{33,35} that is not considered in the model. The underestimation of IEPOXOS and overestimation of tetrols also suggests that Riedel et al.²⁷ may underestimate the organosulfate formation rate constant relative to the tetrol formation rate constant. The PM_{2.5} samples were integrated over 3–11 h sampling time.⁹ Thus, assuming 6 h model processing time is reasonable and within the range of filter measurements.

The predicted speciation between IEPOXOS and tetrols ($\beta = 0.13 \pm 0.05$) is similar to previous laboratory results for bulk solutions that are predominantly bisulfate vs sulfate such as in the work of Eddingsaas et al.¹⁹ ($\beta = 0.09$ for 1.0 M H₂SO₄). Note that $\beta = 0.4$ is used in standard GAMMA¹⁵ and simpleGAMMA¹⁶ and corresponds to the most concentrated bulk solution studied by Eddingsaas et al. (0.1 M H₂SO₄ with 3.0 M Na₂SO₄).¹⁹ Piletic et al.³⁸ predicted a higher rate constant for aqueous IEPOX reaction with sulfate than the value used here from Riedel et al.²⁷ A sensitivity simulation with the organosulfate formation rate constant of Piletic et al.³⁸ resulted in $0.35 < \beta < 0.61$. The third order organosulfate formation rate constants determined by Riedel et al.²⁷ and implemented here are designed to be independent of sulfate concentration. To get the overall rate of reaction, the rate constants are multiplied by the concentration of sulfate and LWC (eq 6). Thus, the effect of differences in sulfate concentration between the laboratory and field conditions is captured in the model. The reactive uptake coefficient of IEPOX (γ_{IEPOX}) using the experimental values of Riedel et al.²⁷ is estimated to be 3.2×10^{-4} on average but ranged between 9.0×10^{-7} and 2.4×10^{-3} . The values overlap with the low end of ranges previously measured for reactive uptake of trans- β -IEPOX on sulfate seed aerosol of varying acidity (2.0×10^{-4} to 7.0×10^{-2}).^{39,40}

Governing Model Processes. The particle-phase reaction rate (eq 6, Table 1) and physical parameters used in simpleGAMMA and CMAQ are intentionally made the same in this study to eliminate potential differences in predictions due to different chemical parameter choices. The difference

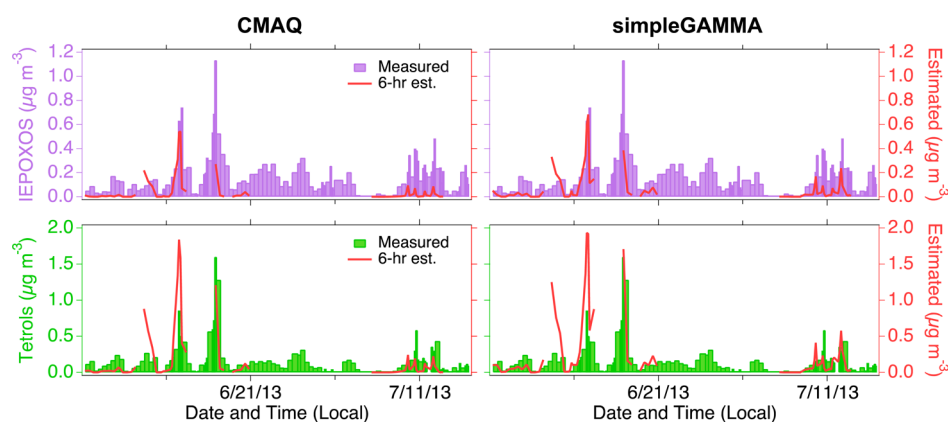


Figure 2. Time traces of IEPOXOS and tetrols as predicted by simpleGAMMA and CMAQ-box model (solid bars) in comparison with measurements (solid red line) during 2013 SOAS.

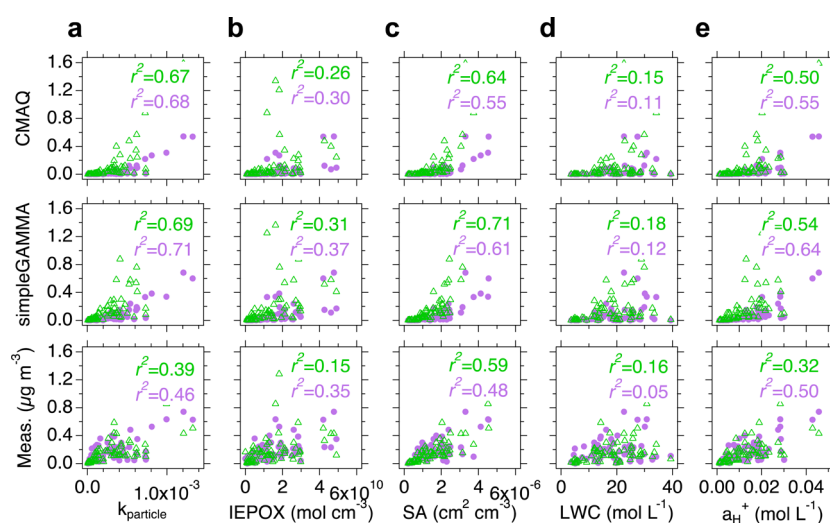


Figure 3. Correlation between estimated IEPOXOS (solid purple circle) and tetrols (open green triangle) by CMAQ and simpleGAMMA in $\mu\text{g m}^{-3}$ as well as measured tracers during 2013 SOAS at LRK with model variables: (a) k_{particle} , (b) gas-phase IEPOX (mol cm^{-3}), (c) aerosol surface area (SA, $\text{cm}^2 \text{cm}^{-3}$), (d) liquid water content (LWC, mol L^{-1}), and (e) a_{H^+} (mol L^{-1}). Both models estimate the tracers for 6 h processing time.

between the two models lies in the formulation of the uptake of IEPOX. CMAQ-box represents the uptake of IEPOX as an irreversible heterogeneous process onto a particle surface (k_{het}), whereas simpleGAMMA calculates equilibrium mass transfer between the gas and aerosol phases according to Henry's Law at each time step. SimpleGAMMA allows for unreacted IEPOX in the aqueous particle phase while CMAQ-box does not. The reactive uptake formulation of CMAQ does, however, allow for potential mass transfer limitations in the particle that would result in a surface-based reaction instead of reaction in the bulk. Figure 1 indicates that simpleGAMMA tends to give slightly higher estimates of SOA mass than CMAQ-box. Differences in predictions between the two models were attributed to different dependencies on the representation of aerosol size. Specifically, CMAQ-box explicitly depends on aerosol SA while simpleGAMMA depends on aerosol volume. The SA, liquid volume (w_L), and radius input (r_p) for both models were estimated from observations of dry SA, mass concentrations, and dry size distributions. Uncertainty in corrections of those quantities for aerosol water using thermodynamic models could result in slight inconsistencies in physical properties; especially, since atmospheric aerosols are not monodisperse and uniform particles, surface-area-weighted and volume-weighted proper-

ties may be different.⁴¹ simpleGAMMA resulted in higher aerosol concentrations than CMAQ-box when $\frac{3w_L}{SA \cdot r_p}$ was greater than 1 which occurred in all but three cases. When $\frac{3w_L}{SA \cdot r_p} = 1$, simpleGAMMA and CMAQ-box algorithms yield the same predictions of total IEPOX-derived aerosol. Thus, higher simpleGAMMA predictions can be attributed to its higher dependency on aerosol volume (w_L).

Strong correlations ($r^2 \sim 0.7$) are found between k_{particle} and estimated tracers, and moderate correlations are found for k_{particle} and measured tracers (r^2 0.4–0.5) (Figure 3a). In addition, moderate correlations are also found between sulfate and estimated and measured tracers (Table 2). IEPOXOS formation is governed by $k_{\text{H}^+, \text{SO}_4^{2-}}$ (rate constant for $[\text{H}^+] \cdot [\text{SO}_4^{2-}]$). Marais et al.⁴² reported that effect of sulfate on a_{H^+}

Table 2. Correlation Values (r^2) of IEPOXOS and Tetrols with Aerosol Sulfate Measured by ACSM

| | simpleGAMMA | CMAQ-box | measurements |
|---------|-------------|----------|--------------|
| IEPOXOS | 0.48 | 0.36 | 0.36 |
| tetrols | 0.54 | 0.41 | 0.35 |

and volume leads to a strong correlation between IEPOX SOA and sulfate measurements. Correlation between k_{particle} and IEPOX SOA tracers in this work suggests that the rate of particle-phase reaction, indicated by k_{particle} , plays an important role in model predictions. This is consistent with Marais et al.,⁴² while in contrast with observations of no correlation between IEPOX-OA factor and a_{H^+} from Look Rock⁹ and Centerville¹¹ ground sites during 2013 SOAS campaign. The lack of correlation between IEPOX SOA and a_{H^+} in previous studies might be due to the fact that a_{H^+} from the field measurements was estimated based on ion balances and molar ratios of dry aerosol and did not use a thermodynamic model.³⁷ In addition, previous estimates of a_{H^+} did not consider how organic compounds occupy particle volume, thus diluting a_{H^+} (SI Table S2).

Local gas-phase IEPOX is weakly correlated with tracer masses estimated by CMAQ ($r^2 \sim 0.3$) and simpleGAMMA ($r^2 \sim 0.3\text{--}0.4$) (Figure 3b). Small differences in correlation values indicate that gas-phase IEPOX input plays a similar role in each model. The weak correlation is consistent with ambient data and indicates that there is little correlation between gas-phase IEPOX and the measured tracers ($r^2 \sim 0.15\text{--}0.35$), likely because it is not a limiting factor.

Investigation of the roles of SA and a_{H^+} , as illustrated in Figures 3(c) and (e), suggests that they could be limiting factors for IEPOXOS and tetrol formation in simpleGAMMA, CMAQ, and the ambient atmosphere. SA and a_{H^+} are correlated with tracers estimated by both models ($r^2 \sim 0.5\text{--}0.7$) and moderately correlated with the measurements ($r^2 \sim 0.3\text{--}0.5$). On the contrary, aerosol volume does not correlate ($r^2 \leq 0.2$) with tracers from model predictions or field observations (SI Figure S4b). Further, we evaluate the significances of k_{particle} and SA variables to SOA tracers (IEPOXOS and tetrol) predicted by CMAQ-box model, and a_{H^+} and sulfate variables to k_{particle} through multivariate regression analysis. The results reaffirm that k_{particle} and SA are significant (p -value < 0.05) to IEPOXOS and tetrol predictions as well as a_{H^+} and SO_4^{2-} to k_{particle} (SI Table S5). These suggest the importance of a_{H^+} , SA, and SO_4^{2-} to the prediction of the SOA tracers. Despite simpleGAMMA not having an explicit dependence on SA, it shows similar behavior to both CMAQ-box and the ambient data in terms of a strong correlation of predictions with SA, but not volume. SI Figure S5a shows a strong correlation between sulfate and SA ($r^2 = 0.75$) but weaker correlation with aerosol volume ($r^2 \sim 0.4$). This suggests that the sulfate concentration in the fine aerosol may more strongly dictate SA than volume, because its size distribution is at the upper range of fine aerosol.⁴³

In addition to sulfate and a_{H^+} , aqueous-phase chemistry in both models is driven by aerosol liquid water content. Interestingly, no correlation ($r^2 \leq 0.2$) is found between estimated and measured tracers and aerosol liquid water content (Figure 3d) and RH (SI Figure S4a), which is consistent with field observations.^{9,11} Aerosol liquid water content is also not correlated ($r^2 \sim 0.1$) with the dry aerosol volume from measurements and the estimated wet aerosol volume as shown in SI Figures S6(a) and (d), respectively. This is consistent with field observations at Look Rock⁹ suggesting that LWC might not be a limiting factor for IEPOX SOA production at this site.

The low correlations ($r^2 \sim 0.3\text{--}0.4$) between LWC and SA, and LWC and sulfate (SI Figures S6(d) and (e) respectively) can be explained in terms of their temporal variability. Sulfate is a regional pollutant with a minimal diurnal variation (SI Figure

S7), while RH and LWC have pronounced diurnal cycles; given this and that LWC scales linearly with sulfate amount and exponentially with RH, we expect RH variability to drive the LWC variability. To support this, we repeat the correlation calculation between LWC and sulfate for narrow RH ranges (SI Figure S8a) and find r^2 to be much higher (0.5–0.6). Similarly, a slightly stronger correlation is found between LWC versus SA for narrow RH ranges ($r^2 \sim 0.5\text{--}0.6$; SI Figure S8b), suggesting an impact of RH variability to SA variability. A stronger correlation between LWC and a_{H^+} at the lower RH range ($r^2 = 0.90$; SI Figure S8c) compared to that at the higher RH range ($r^2 \sim 0.5$) indicates a significant impact of RH on a_{H^+} . In addition, LWC can serve to dilute a_{H^+} .

Effect of Sulfate Reduction on Estimated SOA.

Ambient data and modeling in the previous section suggests that sulfate plays a significant role in IEPOX SOA formation through its effects on SA and particle-phase reaction rate. Using the CMAQ model, Pye et al.¹³ showed a SO_x reduction resulted in a more significant reduction of isoprene-derived SOA compared than a similar NO_x reduction. Furthermore, SO_x reductions have also been observed to be correlated with organic aerosol in ambient measurements in the SE US.^{44,45}

In this study, we find that a 25% sulfate reduction results in a $\sim 70\%$ decrease in the predicted tetrol concentration and $\sim 75\%$ decrease in IEPOXOS (Figure 4). Due to the decrease of

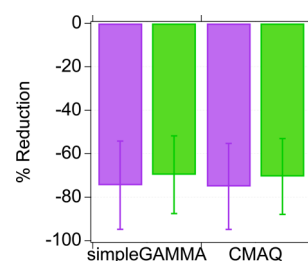


Figure 4. Reduction of (a) IEPOXOS (purple), and (b) tetrols (green) mass concentration estimated by CMAQ and simpleGAMMA as a result of 25% reduction in sulfate. Vertical bars represent 1-standard deviation of average percent reduction of each model prediction.

sulfate, the proton activity (a_{H^+}) decreases up to 64%. These results indicate sulfate (a proxy for SO_x) reductions are about a factor of 2 more effective in reducing IEPOX SOA than was found by Pye et al.¹³ (see figure associated with abstract), which might be related to the examination of different years with different aerosol loadings (2006 in Pye et al.¹³ vs 2013 here) and the higher rate constant for reaction with sulfate in this work as well as the difference in using a box model versus 3-D chemical transport model. Figure 4 indicates the IEPOXOS concentration is slightly more sensitive to changes in sulfate than the tetrol concentration. Reductions in sulfate aerosol mass do not change LWC (in mol L^{-1} of aerosol) substantially ($\sim 13\%$ reduction; SI Figure S9) since RH is more influential to LWC than sulfate.

Atmospheric Significance. Previous studies have observed large discrepancies between model estimations and measurements of organic aerosol⁴⁶ and in particular IEPOX SOA.¹⁴ Improvements in model representations of SOA are important for environmental policy and management, and for establishing an effective predictive capability, which is the ultimate goal of atmospheric chemistry research.⁴⁷ This study provides a comparison between two model estimates and

measurements of IEPOX SOA (i.e., IEPOXOS and tetrols). IEPOXOS and tetrols observed at the SOAS-LRK site are estimated well by simpleGAMMA and CMAQ-box ($r^2 \sim 0.6$). The particle-phase reaction rate computed from the acids and nucleophile concentration in the particle, influences IEPOXOS and tetrol formation ($r^2 \sim 0.6$ – 0.7 in the models). In addition, aerosol physical characteristics (i.e., surface area) are observed to have strong correlations with aerosol sulfate and IEPOX aerosol tracer concentrations in both models and measurements. The significant reduction of IEPOX SOA from a 25% reduction of SO_x emission (implemented as a sulfate aerosol reduction) observed in this study highlights the nonlinear (synergistic) interactions between anthropogenic and biogenic emissions in the atmosphere.

In locations where aqueous-phase glyoxal chemistry may also play a significant role in isoprene SOA formation, for instance in urban environments, simpleGAMMA should be further evaluated as it includes the mechanism of SOA formation from glyoxal uptake.¹⁶ GEOS-Chem⁴² also includes aqueous-phase glyoxal chemistry in its representation of isoprene SOA and this may be the reason that the total isoprene-SOA in GEOS-Chem is less sensitive to SO_x (abstract figure) than individual IEPOX SOA tracers, such as 2-methyltetrols and IEPOXOS. Furthermore, a full-scale chemical transport model calculation may show a more moderate response to emission changes compared to a box model since multiple aerosol pathways would be considered. Estimates with CMAQ that did not consider acid-catalyzed reactive uptake of IEPOX, previously suggested 50% of biogenically derived SOA in the eastern U.S. is controllable.^{4,7} The work here suggests that the estimate is too low since aqueous phase IEPOX SOA is sensitive to SO_x emission changes.

■ ASSOCIATED CONTENT

📄 Supporting Information

The Supporting Information is available free of charge on the ACS Publications website at DOI: 10.1021/acs.est.6b05750.

Tables S1 and S2 list model variables used in this study and their correlations with the predicted and measured SOA tracers. Table S3 provides CMAQ predictions of gas-phase IEPOX and ISOPOOH mixing ratios at LRK site during the 2013 SOAS campaign. Table S4 provides correlation coefficient values and slopes from orthogonal regression linear of estimated and measured tracers. Table S5 provides results of multivariate regression analysis of relationships between the key variables and estimated SOA tracers. Figure S1 shows the effect of adding NH_4^+ protonation reaction with IEPOX in k_{particle} . Figure S2 shows correlation between sulfate measured by the ACSM at LRK site versus those of the ISORROPIA-II output, and the SOA model input. Figure S3 shows fraction of inorganic, organic and liquid water in the aerosol. Figure S4 shows correlation between the estimated and measured tracers and model variables (i.e., RH and aerosol volume). Figure S5 shows correlation between SA and volume with aerosol sulfate concentration. Figure S6 shows correlation between SA and volume measured by SEMs-MCPC, sulfate aerosol measured by ACSM, and estimated proton activity with aerosol liquid water content. Figures S7 and S8 show diurnal trends of sulfate, LWC and RH and relationship between sulfate and LWC at different RH, respectively.

Figure S9 shows effects of SO_4 reduction to proton activity (a_{H^+} and aerosol LWC variables) (PDF)

■ AUTHOR INFORMATION

Corresponding Authors

*(V.F.M.) E-mail: vfm2103@columbia.edu.

*(H.O.T.P.) E-mail: Pye.Havala@epa.gov.

ORCID

Sri Hapsari Budisulistiorini: 0000-0002-5715-9157

Annmarie G. Carlton: 0000-0002-8574-1507

V. Faye McNeill: 0000-0003-0379-6916

Havala O. T. Pye: 0000-0002-2014-2140

Notes

The authors declare no competing financial interest.

■ ACKNOWLEDGMENTS

S.H.B. was supported through Internship/Research Participation Program at the Office of Research and Development, U.S. EPA, administered by the Oak Ridge Institute for Science and Education through an interagency agreement between the U.S. Department of Energy and EPA. The U.S. EPA through its Office of Research and Development supported the research described here. It has been subjected to Agency administrative review and approved for publication, but may not necessarily reflect official Agency policy. V.F.M. acknowledges funding by NSF (award number AGS-1546136). AN was supported in part by the U.S. EPA (grant number R835410) and the Electric Power Research Institute (EPRI). The Surratt Group was supported in part by the U.S. EPA (grant number 835404), the Electric Power Research Institute (EPRI), and the National Oceanic and Atmospheric Administration (NOAA) Climate Program Office's AC4 program (Award no. NA13OAR4310064).

■ REFERENCES

- (1) IPCC. *Climate Change 2013: The Physical Science Basis, Contribution of Working Group I to the Fifth Assessment Report to the Intergovernmental Panel on Climate Change*, 2013; pp 33–118.
- (2) Zhang, Q.; Jimenez, J. L.; Canagaratna, M. R.; Allan, J. D.; Coe, H.; Ulbrich, I.; Alfarra, M. R.; Takami, A.; Middlebrook, A. M.; Sun, Y. L.; Dzepina, K.; Dunlea, E.; Docherty, K.; DeCarlo, P. F.; Salcedo, D.; Onasch, T.; Jayne, J. T.; Miyoshi, T.; Shimojo, A.; Hatakeyama, S.; Takegawa, N.; Kondo, Y.; Schneider, J.; Drewnick, F.; Borrmann, S.; Weimer, S.; Demerjian, K.; Williams, P.; Bower, K.; Bahreini, R.; Cottrell, L.; Griffin, R. J.; Rautiainen, J.; Sun, J. Y.; Zhang, Y. M.; Worsnop, D. R. Ubiquity and dominance of oxygenated species in organic aerosols in anthropogenically-influenced Northern Hemisphere midlatitudes. *Geophys. Res. Lett.* **2007**, *34*, L13801.
- (3) Goldstein, A. H.; Koven, C. D.; Heald, C. L.; Fung, I. Y. Biogenic carbon and anthropogenic pollutants combine to form a cooling haze over the southeastern United States. *Proc. Natl. Acad. Sci. U. S. A.* **2009**, *106*, 8835–8840.
- (4) Carlton, A. G.; Pinder, R. W.; Bhawe, P. V.; Pouliot, G. A. To What Extent Can Biogenic SOA be Controlled? *Environ. Sci. Technol.* **2010**, *44*, 3376–3380.
- (5) Ford, B.; Heald, C. L. Aerosol loading in the Southeastern United States: reconciling surface and satellite observations. *Atmos. Chem. Phys.* **2013**, *13*, 9269–9283.
- (6) Guenther, A.; Karl, T.; Harley, P.; Wiedinmyer, C.; Palmer, P. I.; Geron, C. Estimates of global terrestrial isoprene emissions using MEGAN (Model of Emissions of Gases and Aerosols from Nature). *Atmos. Chem. Phys.* **2006**, *6*, 3181–3210.

- (7) Carlton, A. G.; Wiedinmyer, C.; Kroll, J. H. A review of Secondary Organic Aerosol (SOA) formation from isoprene. *Atmos. Chem. Phys.* **2009**, *9*, 4987–5005.
- (8) Lin, Y.; Knipping, E. M.; Edgerton, E. S.; Shaw, S. L.; Surratt, J. D. Investigating the influences of SO₂ and NH₃ levels on isoprene-derived secondary organic aerosol formation using conditional sampling approaches. *Atmos. Chem. Phys. Discuss.* **2013**, *13*, 3095–3134.
- (9) Budisulistiorini, S. H.; Li, X.; Bairai, S. T.; Renfro, J.; Liu, Y.; Liu, Y. J.; McKinney, K. A.; Martin, S. T.; McNeill, V. F.; Pye, H. O. T.; Nenes, A.; Neff, M. E.; Stone, E. A.; Mueller, S.; Knote, C.; Shaw, S. L.; Zhang, Z.; Gold, A.; Surratt, J. D. Examining the effects of anthropogenic emissions on isoprene-derived secondary organic aerosol formation during the 2013 Southern Oxidant and Aerosol Study (SOAS) at the Look Rock, Tennessee ground site. *Atmos. Chem. Phys.* **2015**, *15*, 8871–8888.
- (10) Budisulistiorini, S. H.; Canagaratna, M. R.; Croteau, P. L.; Marth, W. J.; Baumann, K.; Edgerton, E. S.; Shaw, S. L.; Knipping, E. M.; Worsnop, D. R.; Jayne, J. T.; Gold, A.; Surratt, J. D. Real-time continuous characterization of secondary organic aerosol derived from isoprene epoxydiols in downtown Atlanta, Georgia, using the Aerodyne Aerosol Chemical Speciation Monitor. *Environ. Sci. Technol.* **2013**, *47*, 5686–5694.
- (11) Xu, L.; Guo, H.; Boyd, C. M.; Klein, M.; Bougiatioti, A.; Cerully, K. M.; Hite, J. R.; Isaacman-VanWertz, G.; Kreisberg, N. M.; Knote, C.; Olson, K.; Koss, A.; Goldstein, A. H.; Hering, S. V.; de Gouw, J.; Baumann, K.; Lee, S.; Nenes, A.; Weber, R. J.; Ng, N. L. Effects of anthropogenic emissions on aerosol formation from isoprene and monoterpenes in the southeastern United States. *Proc. Natl. Acad. Sci. U. S. A.* **2015**, *112*, 37–42.
- (12) Carlton, A. G.; Bhawe, P. V.; Napelenok, S. L.; Edney, E. O.; Sarwar, G.; Pinder, R. W.; Pouliot, G. A.; Houyoux, M. Model representation of secondary organic aerosol in CMAQv4.7. *Environ. Sci. Technol.* **2010**, *44*, 8553–8560.
- (13) Pye, H. O. T.; Pinder, R. W.; Piletic, I. R.; Xie, Y.; Capps, S. L.; Lin, Y.; Surratt, J. D.; Zhang, Z.; Gold, A.; Luecken, D. J.; Hutzell, W. T.; Jaoui, M.; Offenber, J. H.; Kleindienst, T. E.; Lewandowski, M.; Edney, E. O. Epoxide pathways improve model predictions of isoprene markers and reveal key role of acidity in aerosol formation. *Environ. Sci. Technol.* **2013**, *47*, 11056–11064.
- (14) Karambelas, A.; Pye, H. O. T.; Budisulistiorini, S. H.; Surratt, J. D.; Pinder, R. W. Contribution of isoprene epoxydiol to urban organic aerosol: evidence from modeling and measurements. *Environ. Sci. Technol. Lett.* **2014**, *1*, 278–283.
- (15) McNeill, V. F.; Woo, J. L.; Kim, D. D.; Schwi, A. N.; Wannell, N. J.; Sumner, A. J.; Barakat, J. M. Aqueous-phase secondary organic aerosol and organosulfate formation in atmospheric aerosols: a modeling study. *Environ. Sci. Technol.* **2012**, *46*, 8075–8081.
- (16) Woo, J. L.; McNeill, V. F. simpleGAMMA 1.0 – A reduced model of secondary organic aerosol formation in the aqueous aerosol phase (aaSOA). *Geosci. Model Dev.* **2015**, *8*, 1821–1829.
- (17) Surratt, J. D.; Murphy, S. M.; Kroll, J. H.; Ng, N. L.; Hildebrandt, L.; Sorooshian, A.; Szmigielski, R.; Vermeylen, R.; Maenhaut, W.; Claeys, M.; Flagan, R. C.; Seinfeld, J. H. Chemical composition of secondary organic aerosol formed from the photo-oxidation of isoprene. *J. Phys. Chem. A* **2006**, *110*, 9665–9690.
- (18) Lin, Y.; Zhang, Z.; Docherty, K. S.; Zhang, H.; Budisulistiorini, S. H.; Rubitschun, C. L.; Shaw, S. L.; Knipping, E. M.; Edgerton, E. S.; Kleindienst, T. E.; Gold, A.; Surratt, J. D. Isoprene epoxydiols as precursors to secondary organic aerosol formation: Acid-catalyzed reactive uptake studies with authentic compounds. *Environ. Sci. Technol.* **2012**, *46*, 250–258.
- (19) Eddingsaas, N. C.; VanderVelde, D. G.; Wennberg, P. O. Kinetics and products of the acid-catalyzed ring-opening of atmospherically relevant butyl epoxy alcohols. *J. Phys. Chem. A* **2010**, *114*, 8106–8113.
- (20) Surratt, J. D.; Lewandowski, M.; Offenber, J. H.; Jaoui, M.; Kleindienst, T. E.; Edney, E. O.; Seinfeld, J. H. Effect of Acidity on Secondary Organic Aerosol Formation from Isoprene. *Environ. Sci. Technol.* **2007**, *41*, 5363–5369.
- (21) Froyd, K. D.; Murphy, S. M.; Murphy, D. M.; de Gouw, J. A.; Eddingsaas, N. C.; Wennberg, P. O. Contribution of isoprene-derived organosulfates to free tropospheric aerosol mass. *Proc. Natl. Acad. Sci. U. S. A.* **2010**, *107*, 21360.
- (22) Jacob, D. J. Heterogeneous chemistry and tropospheric ozone. *Atmos. Environ.* **2000**, *34*, 2131–2159.
- (23) Schwartz, S. E. *Mass-Transport Considerations Pertinent to Aqueous Phase Reactions of Gases in Liquid-Water Clouds*; Jaeschke, W., Ed.; Chemistry of Multiphase Atmospheric Systems; Springer: Berlin Heidelberg, 1986; Vol. 6, pp 415–471.
- (24) Hanson, D. R.; Ravishankara, A. R.; Solomon, S. Heterogeneous reactions in sulfuric acid aerosols: A framework for model calculations. *J. Geophys. Res.* **1994**, *99*, 3615–3629.
- (25) Gharagheizi, F.; Eslamimanesh, A.; Mohammadi, A. H.; Richon, D. Representation and Prediction of Molecular Diffusivity of Nonelectrolyte Organic Compounds in Water at Infinite Dilution Using the Artificial Neural Network-Group Contribution Method. *J. Chem. Eng. Data* **2011**, *56*, 1741–1750.
- (26) Pye, H. O. T.; Murphy, B. N.; Xu, L.; Ng, N. L.; Carlton, A. G.; Guo, H.; Weber, R.; Vasilakos, P.; Appel, K. W.; Budisulistiorini, S. H.; Surratt, J. D.; Nenes, A.; Hu, W.; Jimenez, J. L.; Isaacman-VanWertz, G.; Misztal, P. K.; Goldstein, A. H. On the implications of aerosol liquid water and phase separation for organic aerosol mass. *Atmos. Chem. Phys.* **2017**, *17*, 343–369.
- (27) Riedel, T. P.; Lin, Y. -; Zhang, Z.; Chu, K.; Thornton, J. A.; Vizuet, W.; Gold, A.; Surratt, J. D. Constraining condensed-phase formation kinetics of secondary organic aerosol components from isoprene epoxydiols. *Atmos. Chem. Phys.* **2016**, *16*, 1245–1254.
- (28) Fountoukidis, C.; Nenes, A. ISORROPIA II: a computationally efficient thermodynamic equilibrium model for K⁺–Ca²⁺–Mg²⁺–NH₄⁺–Na⁺–SO₄²⁻–NO₃⁻–Cl⁻–H₂O aerosols. *Atmos. Chem. Phys.* **2007**, *7*, 4639–4659.
- (29) Nguyen, T. B.; Coggon, M. M.; Bates, K. H.; Zhang, X.; Schwantes, R. H.; Schilling, K. A.; Loza, C. L.; Flagan, R. C.; Wennberg, P. O.; Seinfeld, J. H. Organic aerosol formation from the reactive uptake of isoprene epoxydiols (IEPOX) onto non-acidified inorganic seeds. *Atmos. Chem. Phys.* **2014**, *14*, 3497–3510.
- (30) You, Y.; Renbaum-Wolff, L.; Bertram, A. K. Liquid-liquid phase separation in particles containing organics mixed with ammonium sulfate, ammonium bisulfate, ammonium nitrate or sodium chloride. *Atmos. Chem. Phys.* **2013**, *13*, 11723–11734.
- (31) Guo, H.; Xu, L.; Bougiatioti, A.; Cerully, K. M.; Capps, S. L.; Hite, J. R., Jr.; Carlton, A. G.; Lee, S. H.; Bergin, M. H.; Ng, N. L.; Nenes, A.; Weber, R. J. Fine-particle water and pH in the southeastern United States. *Atmos. Chem. Phys.* **2015**, *15*, 5211–5228.
- (32) Li, Y.; Pöschl, U.; Shiraiwa, M. Molecular corridors and parameterizations of volatility in the chemical evolution of organic aerosols. *Atmos. Chem. Phys.* **2016**, *16*, 3327–3344.
- (33) Isaacman-VanWertz, G.; Yee, L. D.; Kreisberg, N. M.; Wernis, R.; Moss, J. A.; Hering, S. V.; de Sá, S. S.; Martin, S. T.; Alexander, M. L.; Palm, B. B.; Hu, W.; Campuzano-Jost, P.; Day, D. A.; Jimenez, J. L.; Riva, M.; Surratt, J. D.; Viegas, J.; Manzi, A.; Edgerton, E.; Baumann, K.; Souza, R.; Artaxo, P.; Goldstein, A. H. Ambient Gas-Particle Partitioning of Tracers for Biogenic Oxidation. *Environ. Sci. Technol.* **2016**, *50*, 9952–9962.
- (34) Claeys, M.; Graham, B.; Vas, G.; Wang, W.; Vermeylen, R.; Pashynska, V.; Cafmeyer, J.; Guyon, P.; Andreae, M. O.; Artaxo, P.; Maenhaut, W. Formation of Secondary Organic Aerosols Through Photooxidation of Isoprene. *Science* **2004**, *303*, 1173–1176.
- (35) Lopez-Hilfiker, F. D.; Mohr, C.; D'Ambro, E. L.; Lutz, A.; Riedel, T. P.; Gaston, C. J.; Iyer, S.; Zhang, Z.; Gold, A.; Surratt, J. D.; Lee, B. H.; Kurten, T.; Hu, W. W.; Jimenez, J.; Hallquist, M.; Thornton, J. A. Molecular Composition and Volatility of Organic Aerosol in the Southeastern U.S.: Implications for IEPOX Derived SOA. *Environ. Sci. Technol.* **2016**, *50*, 2200–2209.
- (36) Pye, H. O. T.; Luecken, D. J.; Xu, L.; Boyd, C. M.; Ng, N. L.; Baker, K.; Ayres, B. A.; Bash, J. O.; Baumann, K.; Carter, W. P. L.;

Egerton, E.; Fry, J. L.; Hutzell, W. T.; Schwede, D.; Shepson, P. B. Modeling the current and future roles of particulate organic nitrates in the southeastern United States. *Environ. Sci. Technol.* **2015**, *49*, 14195–14203.

(37) Weber, R. J.; Guo, H.; Russell, A. G.; Nenes, A. High aerosol acidity despite declining atmospheric sulfate concentrations over the past 15 years. *Nat. Geosci.* **2016**, *9*, 282–285.

(38) Piletic, I. R.; Edney, E. O.; Bartolotti, L. J. A computational study of acid catalyzed aerosol reactions of atmospherically relevant epoxides. *Phys. Chem. Chem. Phys.* **2013**, *15*, 18065–18076.

(39) Riedel, T. P.; Lin, Y.; Budisulistiorini, S. H.; Gaston, C. J.; Thornton, J. A.; Zhang, Z.; Vizuete, W.; Gold, A.; Surratt, J. D. Heterogeneous reactions of isoprene-derived epoxides: reaction probabilities and molar secondary organic aerosol yield estimates. *Environ. Sci. Technol. Lett.* **2015**, *2*, 38–42.

(40) Gaston, C. J.; Riedel, T. P.; Zhang, Z.; Gold, A.; Surratt, J. D.; Thornton, J. A. Reactive Uptake of an Isoprene-Derived Epoxydiol to Submicron Aerosol Particles. *Environ. Sci. Technol.* **2014**, *48*, 11178–11186.

(41) Ervens, B.; Turpin, B. J.; Weber, R. J. Secondary organic aerosol formation in cloud droplets and aqueous particles (aqSOA): a review of laboratory, field and model studies. *Atmos. Chem. Phys.* **2011**, *11*, 11069–11102.

(42) Marais, E. A.; Jacob, D. J.; Jimenez, J. L.; Campuzano-Jost, P.; Day, D. A.; Hu, W. W.; Krechmer, J. E.; Zhu, L.; Kim, P. S.; Miller, C. C.; Fisher, J. A.; Travis, K.; Yu, K.; Hanisco, T. F.; Wolfe, G. M.; Arkinson, H. L.; Pye, H. O. T.; Froyd, K. D.; Liao, J.; McNeill, V. F. Aqueous-phase mechanism for secondary organic aerosol formation from isoprene: application to the Southeast United States and co-benefit of SO₂ emission controls. *Atmos. Chem. Phys.* **2016**, *16*, 1603–1618.

(43) Sun, Y. L.; Zhang, Q.; Schwab, J. J.; Demerjian, K. L.; Chen, W. N.; Bae, M. S.; Hung, H. M.; Hogrefe, O.; Frank, B.; Rattigan, O. V.; Lin, Y. C. Characterization of the sources and processes of organic and inorganic aerosols in New York city with a high-resolution time-of-flight aerosol mass spectrometer. *Atmos. Chem. Phys.* **2011**, *11*, 1581–1602.

(44) Nguyen, T. K. V.; Capps, S. L.; Carlton, A. G. Decreasing Aerosol Water Is Consistent with OC Trends in the Southeast U.S. *Environ. Sci. Technol.* **2015**, *49*, 7843–7850.

(45) Blanchard, C. L.; Hidy, G. M.; Shaw, S.; Baumann, K.; Egerton, E. S. Effects of emission reductions on organic aerosol in the southeastern United States. *Atmos. Chem. Phys.* **2016**, *16*, 215–238.

(46) De Gouw, J.; Jimenez, J. L. Organic aerosols in the Earth's atmosphere. *Environ. Sci. Technol.* **2009**, *43*, 7614–7618.

(47) National Academies of Sciences, Engineering, and Medicine. *The Future of Atmospheric Chemistry Research: Remembering Yesterday, Understanding Today, Anticipating Tomorrow*, 2016.

Supporting Information

Simulating Aqueous-Phase Isoprene-Epoxydiol (IEPOX) Secondary Organic Aerosol Production During the 2013 Southern Oxidant and Aerosol Study (SOAS)

Sri Hapsari Budisulistiorini^{†,∞,#}, *Athanasios Nenes*^{‡,§,¶,f}, *Annmarie G. Carlton*[‡], *Jason D. Surratt*[∞], *V. Faye McNeill*^{◇,*}, *Havala O. T. Pye*^{†,*}

[†] National Exposure Research Laboratory, US EPA, Research Triangle Park, North Carolina 27711, United States

[∞] Department of Environmental Sciences and Engineering, Gillings School of Global Public Health, University of North Carolina, Chapel Hill, North Carolina 27599, United States

[#] Earth Observatory of Singapore, Nanyang Technological University, Singapore 639798, Singapore

[‡] School of Earth and Atmospheric Sciences, Georgia Institute of Technology, Atlanta, Georgia 30322, United States

[§] School of Chemical and Biomolecular Engineering, Georgia Institute of Technology, Atlanta, Georgia 30322, United States

[¶] Institute of Chemical Engineering Sciences, Foundation for Research and Technology - Hellas, Patras GR-26504, Greece

^f Institute of Environmental Research and Sustainable Development, National Observatory of Athens, Palea Penteli GR-15236, Greece

[‡] Department of Chemistry, University of California, Irvine, California, 92617, United States

[◇] Department of Chemical Engineering, Columbia University, New York, New York 10027, United States

* To whom correspondence should be addressed

Corresponding Author

*(V.F.M) Email: vfm2103@columbia.edu

*(H.O.T.P) Email: Pye.Havala@epa.gov

This supporting information contains 13 pages: 5 tables, 9 figures

Table S1. Variables used in ISORROPIA-II, CMAQ-box and simpleGAMMA models.

| Model Quantity | Units | Source of Estimate |
|-----------------------------------|----------------------------------|---|
| SO ₄ ²⁻ | μmol m ⁻³ | ACSM |
| NO ₃ ⁻ | μmol m ⁻³ | ACSM |
| Cl ⁻ | μmol m ⁻³ | ACSM |
| NH ₄ ⁺ | μmol m ⁻³ | ACSM |
| NH ₃ | μmol m ⁻³ | Ammonia Monitoring Network (AMoN) |
| IEPOX+ISOPOOH | mol cm ⁻³ | HR-ToF-CIMS |
| Aerosol surface area ^a | cm ² cm ⁻³ | SEMS-MCPC |
| RH | fraction | NPS |
| Temperature | °C | NPS |
| LWC ^b | mol L ⁻¹ | ISORROPIA-II |
| SO ₄ ^{2-b} | mol L ⁻¹ | ISORROPIA-II |
| HSO ₄ ^{-b} | mol L ⁻¹ | ISORROPIA-II |
| NH ₄ ^{+b} | mol L ⁻¹ | ISORROPIA-II |
| H ^{+b} | mol L ⁻¹ | ISORROPIA-II |
| pH | | Calculated from ISORROPIA-II outputs |
| wL ^c | cm ³ cm ⁻³ | Calculated from ISORROPIA-II outputs and observed organic aerosol |
| 2-methyltetrols | μg m ⁻³ | GC/EI-MS |
| IEPOX-OS | μg m ⁻³ | UPLC/DAD-ESI-HR-QTOFMS |

^ameasured dry surface area was adjusted for the presence of water using aerosol water predicted by ISORROPIA-II: $A = A_{dry} * \left[\left(\frac{M_{inorganic}}{\rho_{inorganic}} + \frac{M_{org}}{\rho_{org}} + \frac{M_{water}}{\rho_{water}} \right) / \left(\frac{M_{inorganic}}{\rho_{inorganic}} + \frac{M_{org}}{\rho_{org}} \right) \right]^{2/3}$, where M_i is the mass of i per volume of air and ρ_i is the density of the species.

^baqueous-aerosol phase concentrations (C_i) obtained from ISORROPIA-II in mol L⁻¹ were adjusted for the inclusion of organic aerosol (from the ACSM) prior to use in CMAQ and simpleGAMMA box model calculations: $C_i = C_{i,ISORROPIA} wL_{ISORROPIA} / wL$

^ctotal liquid aerosol volume per volume of air including ISORROPIA-II predicted aqueous aerosol (sulfate, water, etc) and organic aerosol: $wL = wL_{ISORROPIA} + M_{org} / \rho_{org}$

Table S2. Correlation values (r^2) between the SOA tracers formed over 12 hours processing time and model variables. Measured SOA tracers are also correlated with the model variables.

| | CMAQ | | Tetrol ($\mu\text{g m}^{-3}$) | | | | CMAQ | | IEPOXOS ($\mu\text{g m}^{-3}$) | | | |
|--|------------------|-----------------|---------------------------------|-----------------|------------------|-----------------|------------------|-----------------|----------------------------------|-----------------|------------------|-----------------|
| | | | simpleGAMMA | | Measured | | | | simpleGAMMA | | Measured | |
| | <i>w/o corr.</i> | <i>w/ corr.</i> | <i>w/o corr.</i> | <i>w/ corr.</i> | <i>w/o corr.</i> | <i>w/ corr.</i> | <i>w/o corr.</i> | <i>w/ corr.</i> | <i>w/o corr.</i> | <i>w/ corr.</i> | <i>w/o corr.</i> | <i>w/ corr.</i> |
| k_{particle} (s^{-1}) | 0.26 | 0.68 | 0.16 | 0.69 | 0.07 | 0.39 | 0.36 | 0.68 | 0.30 | 0.71 | 0.23 | 0.46 |
| IEPOX _(g) (mol cm^{-3}) | 0.53 | 0.30 | 0.40 | 0.31 | 0.15 | 0.15 | 0.55 | 0.30 | 0.47 | 0.37 | 0.35 | 0.35 |
| SA ($\text{cm}^2 \text{cm}^{-3}$) | 0.63 | 0.55 | 0.69 | 0.72 | 0.46 | 0.59 | 0.50 | 0.55 | 0.61 | 0.61 | 0.48 | 0.48 |
| LWC (mol L^{-1}) | 0.06 | 0.11 | 0.01 | 0.19 | 0.01 | 0.16 | 0.12 | 0.11 | 0.07 | 0.12 | 0.08 | 0.05 |
| α_{H^+} (mol L^{-1}) | 0.30 | 0.50 | 0.20 | 0.53 | 0.09 | 0.32 | 0.40 | 0.55 | 0.34 | 0.64 | 0.26 | 0.50 |
| RH | 0.05 | 0.00 | 0.01 | 0.00 | 0.00 | 0.00 | 0.12 | 0.01 | 0.06 | 0.02 | 0.07 | 0.07 |
| Volume ($\text{cm}^3 \text{cm}^{-3}$) | 0.17 | 0.13 | 0.41 | 0.23 | 0.33 | 0.18 | 0.08 | 0.10 | 0.24 | 0.12 | 0.14 | 0.06 |

w/ corr. and *w/o corr.* respectively refer to variables with and without liquid water added to the measured dry-size distribution to get the atmospherically relevant size distribution particles and organics added to the predicted particle volume by ISORROPIA.

Table S3. CMAQ predicted IEPOX and ISOPOOH for the Look Rock, TN site averaged by hour of day for July 2013. CMAQ simulations for this time period are the same as those in Pye et al. (2015).

| Hour | Predicted ISOPOOH | Predicted IEPOX | Predicted IEPOX/ISOPOOH | Predicted ISOPOOH/IEPOX (<i>b</i>) |
|-----------|-------------------|-----------------|-------------------------|--------------------------------------|
| EST=GMT-5 | ppt | ppt | ratio | ratio |
| 0 | 42 | 152 | 3.24 | 0.28 |
| 1 | 39 | 142 | 3.41 | 0.28 |
| 2 | 40 | 139 | 3.77 | 0.29 |
| 3 | 43 | 142 | 4.24 | 0.30 |
| 4 | 42 | 146 | 4.52 | 0.29 |
| 5 | 35 | 133 | 4.08 | 0.26 |
| 6 | 29 | 105 | 3.11 | 0.27 |
| 7 | 40 | 116 | 2.44 | 0.34 |
| 8 | 70 | 162 | 2.25 | 0.43 |
| 9 | 103 | 187 | 1.65 | 0.55 |
| 10 | 131 | 198 | 1.36 | 0.66 |
| 11 | 154 | 216 | 1.33 | 0.71 |
| 12 | 173 | 248 | 1.40 | 0.70 |
| 13 | 187 | 282 | 1.53 | 0.66 |
| 14 | 199 | 324 | 1.67 | 0.61 |
| 15 | 187 | 345 | 1.83 | 0.54 |
| 16 | 183 | 336 | 1.84 | 0.54 |
| 17 | 164 | 278 | 1.78 | 0.59 |
| 18 | 134 | 207 | 1.70 | 0.65 |
| 19 | 109 | 167 | 1.66 | 0.65 |
| 20 | 86 | 153 | 1.91 | 0.56 |

| Hour | Predicted ISOPOOH | Predicted IEPOX | Predicted IEPOX/ISOPOOH | Predicted ISOPOOH/IEPOX (<i>b</i>) |
|------|-------------------|-----------------|-------------------------|--------------------------------------|
| 21 | 65 | 143 | 2.25 | 0.46 |
| 22 | 55 | 151 | 2.59 | 0.36 |
| 23 | 48 | 163 | 3.01 | 0.29 |

Table S4. Correlations of estimated and measured IEPOXOS and tetrols.

| Estimated tracer | simpleGAMMA | | | CMAQ-box | | |
|------------------|-------------|-------------|-------------|----------|-------------|-------------|
| | r^2 | Slope | | r^2 | Slope | |
| | | t = 12 h | t = 6 h | | t = 12 h | t = 6 h |
| IEPOXOS | 0.60 | 1.04 ± 0.09 | 0.52 ± 0.04 | 0.57 | 0.74 ± 0.08 | 0.37 ± 0.04 |
| Tetrols | 0.53 | 3.25 ± 0.30 | 1.51 ± 0.14 | 0.50 | 2.27 ± 0.25 | 1.14 ± 0.12 |

Table S5. Multivariate regression analysis of relationships between k_{particle} and SA to SOA tracers prediction (IEPOXOS and tetrols) as well as between a_{H^+} and SO_4^{2-} to k_{particle} .

| | r^2 | p-value |
|-----------------------|-------|-------------------------|
| Equation S1: IEPOXOS | 0.70 | |
| Intercept | | 6.27 x 10 ⁻⁶ |
| k_{particle} | | 8.51 x 10 ⁻⁷ |
| SA | | 4.66 x 10 ⁻² |
| Equation S2: Tetrol | 0.73 | |
| Intercept | | 1.25 x 10 ⁻⁷ |

| | r^2 | p-value |
|-----------------------------|-------|------------------------|
| $k_{particle}$ | | 1.99×10^{-5} |
| SA | | 5.19×10^{-4} |
| Equation S3: $k_{particle}$ | 0.89 | |
| Intercept | | 2.11×10^{-4} |
| a_{H^+} | | 6.25×10^{-19} |
| SO_4 | | 2.82×10^{-5} |

Multivariate regression models are:

$$IEPOXOS = a + b \cdot k_{particle} + c \cdot SA \quad (S1)$$

$$tetrol = a + b \cdot k_{particle} + c \cdot SA \quad (S2)$$

$$k_{particle} = a + b \cdot a_{H^+} + c \cdot SO_4 \quad (S3)$$

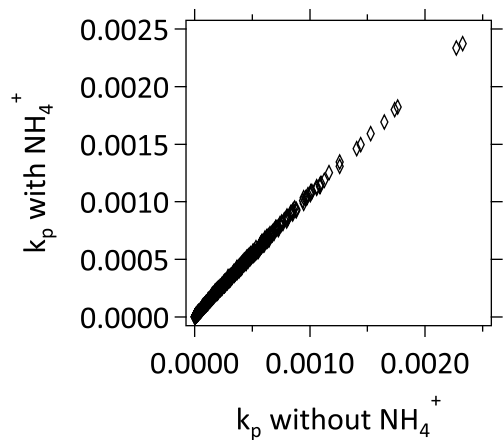


Figure S1. Effect of adding NH_4^+ protonation reaction with IEPOX in k_{particle} (s^{-1}) is negligible as showed by slope of 1.05 for both CMAQ and simpleGAMMA.

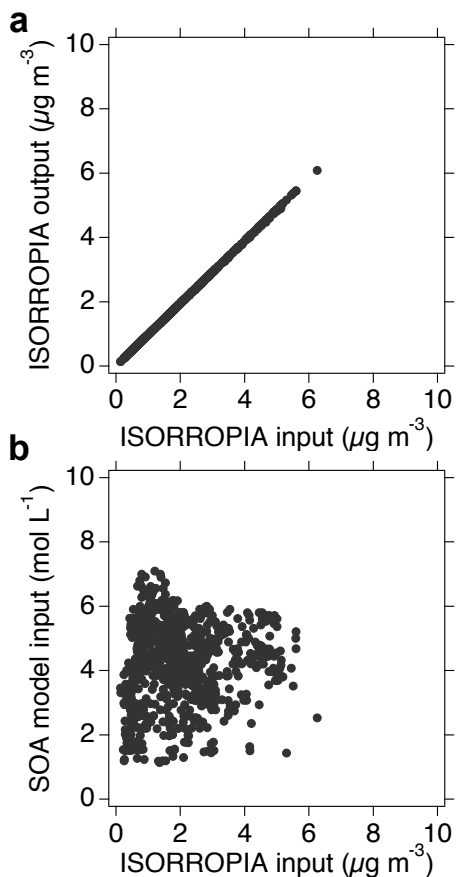


Figure S2. Scatterplots of $[\text{SO}_4^{2-}]$ measured by the ACSM at LRK site (x-axis) versus (a) output of the ISORROPIA-II, and (b) input used in the SOA model (CMAQ and simpleGAMMA). Nucleophile concentration, for instance SO_4^{2-} , used as input in the SOA model considers

contribution of other inorganic ions and organics, as described in the footnote of Table S1. Thus, the values are different from SO_4^{2-} measured by ACSM.

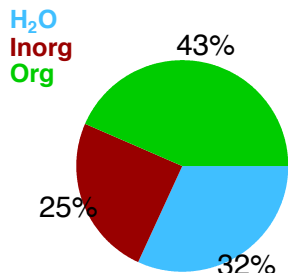


Figure S3. Fraction of inorganic (red), organic (green) and liquid water (blue) in the aerosol.

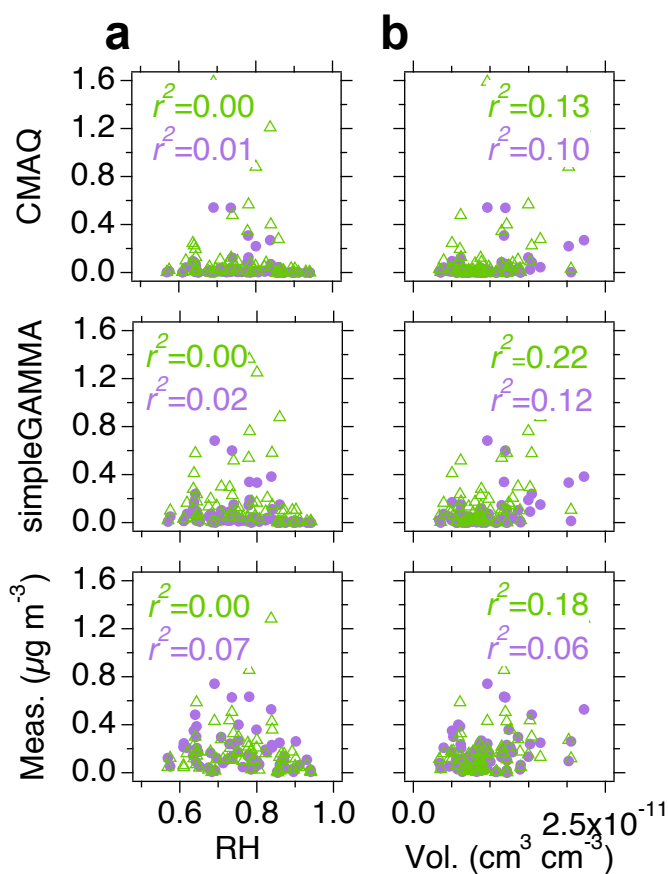


Figure S4. Correlation between estimated IEPOXOS (solid purple circle) and tetrols (open green triangle) by CMAQ and simpleGAMMA in $\mu\text{g m}^{-3}$ as well as measured tracers during 2013 SOAS at LRK with model variables: (a) relative humidity (RH) and (b) aerosol volume (Vol., $\text{cm}^3 \text{cm}^{-3}$). RH is on average 0.77 ± 0.10 during the entire SOAS campaign.

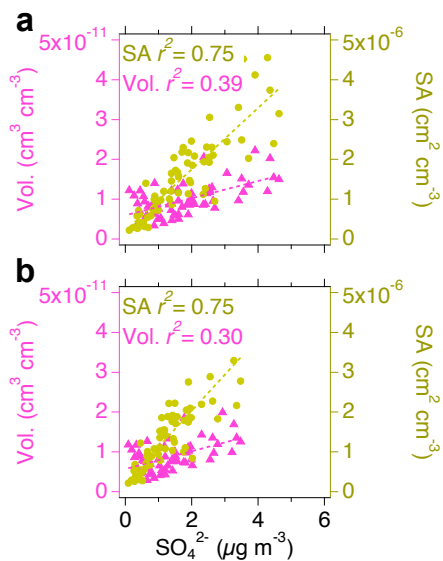


Figure S5. Correlation between aerosol surface area (SA) and liquid volume with sulfate mass concentration from ACSM measurements for (a) base case and (b) sulfate reduction scenarios. Reduction of sulfate does not impact correlation between sulfate, SA and volume.

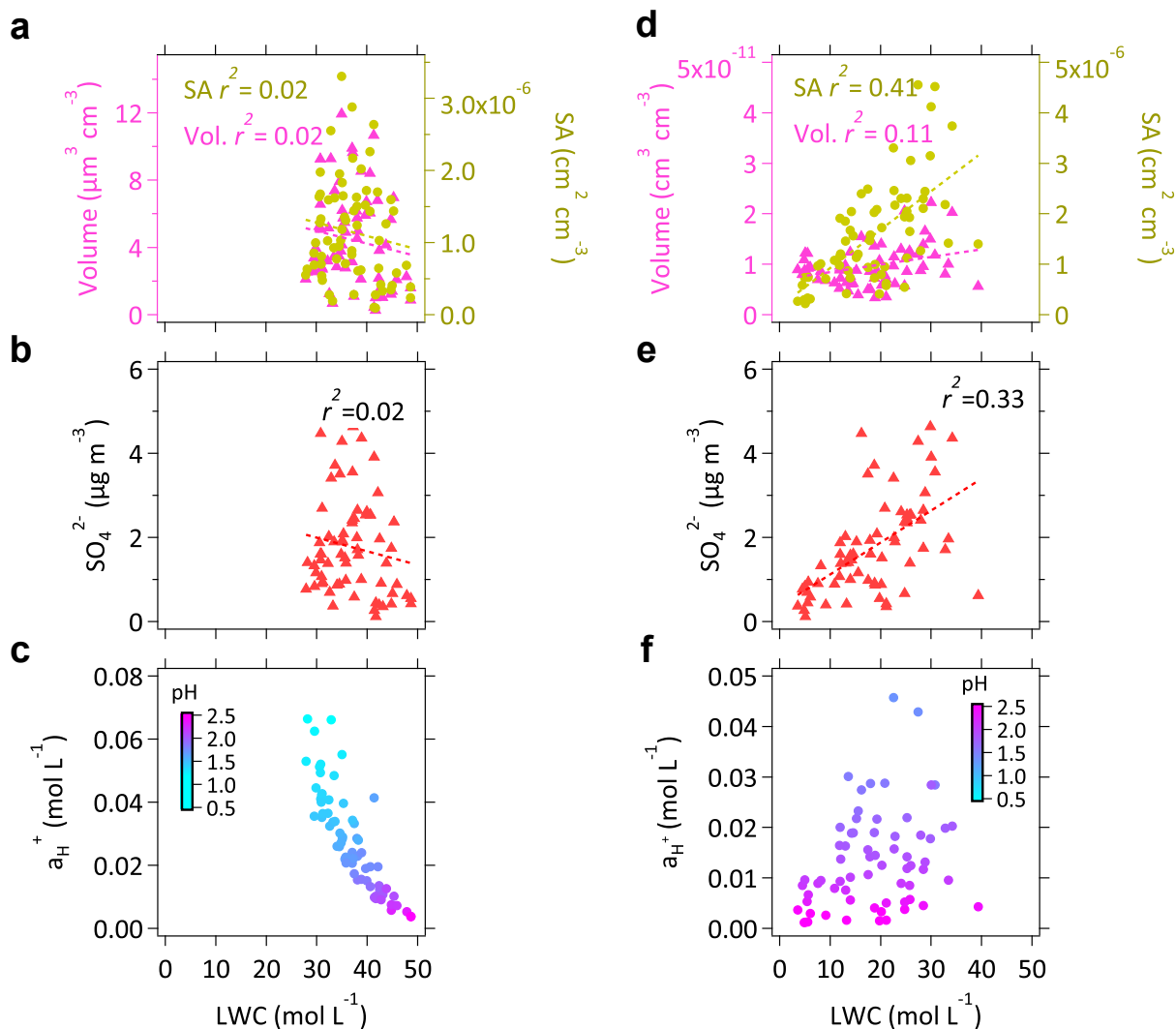


Figure S6. Dry aerosol surface area (SA) and volume measured by SEMS-MCPC (a), and sulfate aerosol measured by ACSM (b) show no relationship with estimated aerosol liquid water directly from ISORROPIA-II (excluding organic aerosol), whereas estimated proton activity (a_{H^+}) has a negative relationship (c). Aerosol SA and volume determined by SEMS-MCPC, ISORROPIA-II, and observed organic aerosol information (d), sulfate aerosol measured by ACSM (e), and estimated a_{H^+} (f) show a relationship with estimated aerosol liquid water when water, organic aerosol, and inorganic aerosol are properly included.

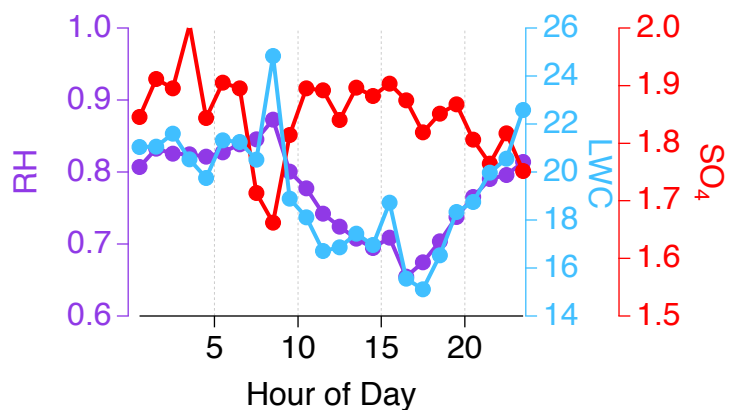


Figure S7. Diurnal trends of RH, LWC and sulfate at LRK site.

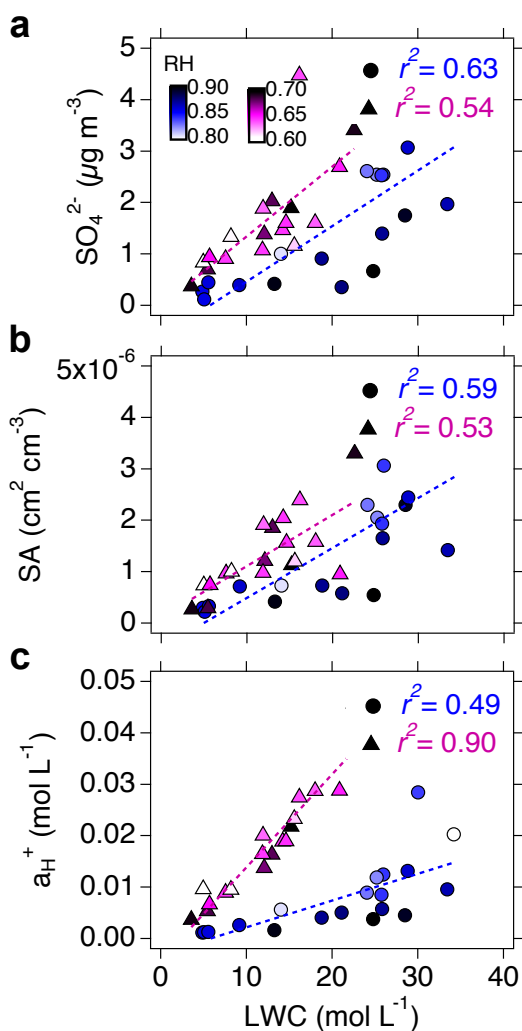


Figure S8. Scatterplots of (a) sulfate (SO_4^{2-}), (b) aerosol surface area (SA), and (c) acidity (a_H^+) versus LWC classified for RH ranges of 0.6 – 0.7 and 0.8 – 0.9.

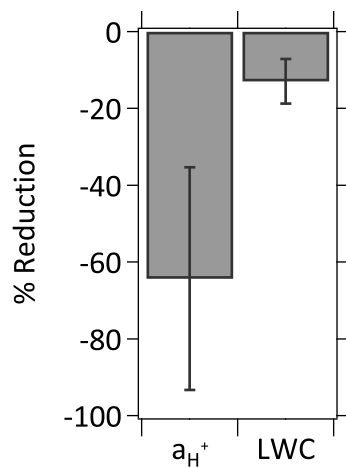


Figure S9. Effects of SO_4^{2-} reduction to proton activity (a_{H^+}) and aerosol liquid water content (LWC) variables are presented as average percentage of changes. Vertical bar shows one standard deviation of the average change percentage. Large changes are found in a_{H^+} variable; however, the variability is large as well. On the other hand, LWC variable does not change significantly.